

Cofacial Bisorganometallic Diporphyrins: Synthetic Control in Proton Reduction Catalysis

James P. Collman,* Yunkyong Ha, Paul S. Wagenknecht, Michel-Angel Lopez,† and Roger Guillard†

Contribution from the Department of Chemistry, Stanford University, Stanford, California 94305

Received March 29, 1993*

Abstract: A series of cofacial bisorganometallic diporphyrin complexes, $M_2^{III/III}R_2DPB$ ($M = Ru, Os$; $R =$ methyl, *p*-tolyl, 3,5-bis(trifluoromethyl)phenyl; $DPB =$ diporphyrinatobiphenylene), has been synthesized by addition of the corresponding Grignard reagents to the dication of the dimetallodiporphyrins. These paramagnetic compounds have been characterized by 1H NMR, cyclic voltammetry, UV-vis, and mass spectrometry. Quantitative two-electron chemical reduction of paramagnetic $M_2^{III/III}R_2DPB$ complexes produces diamagnetic species, $[M_2^{II/II}R_2DPB]^{2-}$; subsequent protonation with suitable acids results in dihydrogen evolution. The overall processes were investigated with 1H NMR. These complexes were examined as possible electrocatalysts for proton reduction by employing mercury-pool electrodes. Acids with a wide range of pK_a values were employed to measure the basicity of these catalysts. Relative overpotentials have been estimated from these pK_a values and the reduction potentials of these cofacial dimetallodiporphyrin complexes. Plausible catalytic proton reduction pathways involving either dihydrogen complexes or dihydrides are discussed.

Introduction

A search for molecular electrode catalysts for proton reduction and an understanding of the underlying reaction mechanisms are interesting problems. Efficient catalysts for this $2 e^-$ reduction occur naturally in the hydrogenase enzymes; these processes have been scrutinized but detailed mechanisms are as yet unknown.¹ A variety of abiological methods for producing dihydrogen have also been investigated² because H_2 has been proposed as an alternative fuel.³ However, electrochemical production of dihydrogen is far more expensive than conventional fuels,⁴ in part due to the inefficiency of the abiological methods. Typically, large overpotentials are required to reduce protons to H_2 . These overpotentials result in inefficient, poor energy conversion.

Spiro and Espenson have developed homogeneous transition metal catalysts for electrochemical proton reduction with relatively low overpotentials.^{5,6} Utilizing cobalt(I) porphyrins and cobaloxime (bis(dimethylglyoximate)cobalt(I) anions, respectively, they showed that dihydrogen is produced in aqueous acidic solution when electrons are provided from a sacrificial electron donor or an electrode. Parallel unimetallic and bimetallic mechanisms were established for dihydrogen production by these catalysts.

Bitterwolf and Mueller-Westerhoff have studied H_2 evolution by protonation of dinuclear systems such as bridged bismetal-locenes.^{7,8} Two mechanisms were proposed to explain this proton reduction. A mechanism requiring both metal centers was

suggested for the simultaneous, reductive H_2 elimination reaction from the two protonated metal centers.^{7a,b,8} Another mechanism was introduced later by Norton, involving a unimetallic process in which the second protonation occurs at a metal hydride site rather than the other metal anion center.^{9a}

To design efficient electrocatalysts for proton reduction, an understanding of the mechanisms for the H_2 evolution reaction is necessary. Using metalloporphyrin hydrides, we previously demonstrated that H_2 can be evolved either from the reaction involving protonation at a single metal hydride or from a bimolecular reaction between two metal hydrides. The reaction mechanism involving a single metal center was substantiated by the observation of dihydrogen complex formation upon protonation of an anionic metal hydride, followed by solvent displacement of H_2 .^{10,11} On the other hand, when the anionic metalloporphyrin hydrides were oxidized at an electrode, dihydrogen was produced in a bimolecular reductive elimination. Cyclic voltammetry and double potential step chronoamperometry demonstrated that the kinetics of $K[Ru(OEP)(THF)(H)]$ decomposition (accompanied by H_2 evolution) upon oxidation is consistent with a bimolecular mechanism.¹² It is this bimolecular reductive elimination of dihydrogen from two metalloporphyrin hydrides that we set out to exploit in the current study.

Previously, we suggested that sensible modification of the central metal, axial ligands, and porphyrin geometry could lead to the design of more efficient proton reduction catalysts.¹² Our current study addresses three points. (1) Can we prepare bimetallic complexes with two available metal coordination sites

* Present address: Université de Bourgogne, Laboratoire de Synthèse Organométallique Associé au C.N.R.S. (URA 33), Faculté des Sciences "Gabriel", 6, Boulevard Gabriel, 21100 Dijon Cedex, France.

† Abstract published in *Advance ACS Abstracts*, September 1, 1993.

(1) Schlegel, H. G.; Schneider, K. *Hydrogenases: Their Catalytic Activity, Structure and Function*; Schlegel, H. G., Schneider, K., Eds.; Verlag: Erich Goltze KG: Göttingen, 1978; pp 15-44.

(2) (a) For a review, see: Koelle, U. *New J. Chem.* **1992**, *16*, 157-169. (b) Efros, L. L.; Thorp, H. H.; Brudvig, G. W.; Crabtree, R. H. *Inorg. Chem.* **1992**, *31*, 1722-1724.

(3) Gregory, D. P.; Tsaros, C. L.; Arora, J. L.; Nevrekar, P. *Hydrogen: Production and Marketing*; Smith, W. N., Santangelo, J. G., Eds.; ACS Symposium Ser. 116; American Chemical Society: Washington, DC 1980; pp 1-26, 33-44.

(4) Wendi, H. *Electrochemical Hydrogen Technologies: Electrochemical Production and Combustion of Hydrogen*; Wendi, H., Ed.; Elsevier: Amsterdam, 1990.

(5) (a) Kelleu, R. M.; Spiro, T. G. *Inorg. Chem.* **1985**, *24*, 2373-2377. (b) Kelleu, R. M.; Spiro, T. G. *Inorg. Chem.* **1985**, *24*, 2378-2382.

(6) (a) Connolly, P.; Espenson, J. H. *Inorg. Chem.* **1986**, *25*, 2684-2688. (b) Chao, T.-H.; Espenson, J. H. *J. Am. Chem. Soc.* **1978**, *100*, 129-133.

(7) (a) Bitterwolf, T. E.; Ling, A. C. *J. Organomet. Chem.* **1973**, *57*, C15-C18; **1981**, *215*, 77-86. (b) Bitterwolf, T. E. *J. Organomet. Chem.* **1983**, *252*, 305-316. (c) Bitterwolf, T. E.; Spink, W. C.; Rausch, M. D. *J. Organomet. Chem.* **1989**, *363*, 189-195. (d) Bitterwolf, T. E.; Raghuvver, K. S. *Inorg. Chim. Acta* **1990**, *172*, 59-64.

(8) Mueller-Westerhoff, U. T.; Nazzari, A. *J. Am. Chem. Soc.* **1984**, *106*, 5381-5382.

(9) (a) Kristjánssdóttir, S. S.; Norton, J. R. *Transition Metal Hydrides: Recent Advances in Theory and Experiment*; Dedieu, A., Ed.; VCH Publishers: New York, 1991; pp 309-360. (b) Tilset, M. *J. Am. Chem. Soc.* **1992**, *114*, 2740-2741 and references therein.

(10) Collman, J. P.; Wagenknecht, P. S.; Hembre, R. T.; Lewis, N. S. *J. Am. Chem. Soc.* **1990**, *112*, 1294-1295.

(11) Collman, J. P.; Wagenknecht, P. S.; Hutchison, J. E.; Lewis, N. S.; Lopez, M.-A.; Guillard, R.; L'Her, M.; Bothner-By, A. A.; Mishra, P. K. *J. Am. Chem. Soc.* **1992**, *114*, 5654-5664.

(12) Collman, J. P.; Wagenknecht, P. S.; Lewis, N. S. *J. Am. Chem. Soc.* **1992**, *114*, 5665-5673.

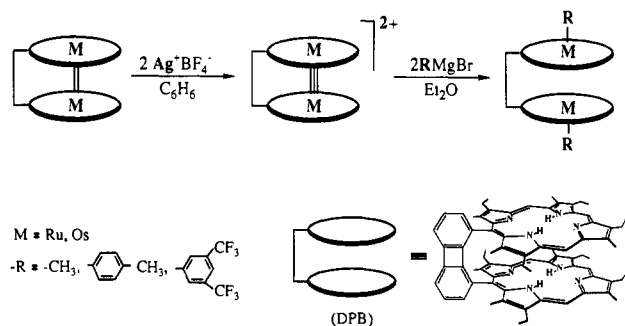


Figure 1. Synthesis scheme of cofacial bisorganometallic diporphyrin complexes.

cofacially disposed? (2) By modification of the central metal and axial ligands, can we affect the overpotential? (3) Does such a cofacial disposition of metal centers result in an enhanced rate of proton reduction?

Herein, we report that specially designed cofacial bisorganometallic diporphyrins can serve as proton reduction catalysts. The intermediates produced by chemical reduction along the proton reduction pathway have been characterized by 1H NMR. The electrochemical properties of these metalloporphyrins have been studied with cyclic voltammetry at Pt electrodes. A wide range of catalyst reduction potentials has been achieved by systematic variation of the metal centers and axial ligands of the cofacial dimetalloporphyrins. The catalytic proton reduction activities of these complexes have been investigated with use of mercury-pool electrodes. Several acids, with a wide range of pK_a values, have been employed to estimate the basicity of these anionic catalysts. Finally, the issue of overpotentials in proton reduction by these metalloporphyrins is discussed and plausible pathways for the overall reaction are proposed.

Results

Syntheses of Cofacial Bisorganometallic Diporphyrin Complexes, M_2R_2DPB . The series of compounds M_2R_2DPB ($M = Ru, Os$; $R = CH_3, p-C_6H_4CH_3, 3,5-(CF_3)_2C_6H_3$) was prepared in two steps from the corresponding metal-metal bonded dimers, M_2DPB (Figure 1). Cofacial metalloporphyrin dimers, Ru_2DPB ^{13a} and Os_2DPB ^{13b} were synthesized according to literature procedures. The chemical and physical properties of these cofacial dimetalloporphyrins are very similar to their respective monomeric metalloporphyrin dimers, $[Ru(OEP)]_2$ and $[Os(OEP)]_2$.¹⁴ Oxidation of the paramagnetic cofacial metalloporphyrin dimers by 2 equiv of Ag^+ yields diamagnetic dimer dications. Presumably, the dimer dications have a metal-metal triple bond with all d electrons paired according to the molecular orbital diagram in Figure 2.¹⁵

The cofacial dimetalloporphyrins with alkyls and aryls on the outer faces of the porphyrin planes were obtained by adding the corresponding Grignard reagent to the dication of the dimetalloporphyrins (Figure 1). Purification by chromatography in an inert atmosphere resulted in M_2R_2DPB complexes, which were characterized by 1H NMR, UV-vis, mass spectrometry, and cyclic voltammetry. Better yields were usually obtained and purifications were simpler compared with the monomeric $M(R)(OEP)$ systems.¹⁶ For example, the formation of $M^{III}(R)(OEP)$ is usually accompanied by the formation of side products

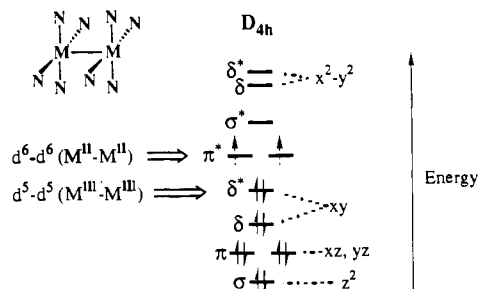


Figure 2. Qualitative MO scheme for the metal-metal bonds of Ru(II) and Os(II) dimers and Ru(III) and Os(III) dimer dications.

such as $M^{IV}(R)_2(OEP)$ whereas double alkylation on one metal center is not seen in the DPB complexes.

Characterization of M_2R_2DPB . Neutral M_2R_2DPB complexes are paramagnetic $d^5 M(III)$ dinuclear systems, displaying contact-shifted 1H NMR signals (e.g., from 98 to -77 ppm in $Ru_2(p-C_6H_4CH_3)_2DPB$) at room temperature. Axial ligand resonances as well as those of the methyl and methylene groups on the β -pyrrolic porphyrin positions are significantly contact-shifted.¹⁷ Although the signals are slightly broadened, all the peaks are assignable and confirm the suggested structures of the complexes.¹⁸ Metal-metal multiple bonds do not seem to be present in the dialkyl or diaryl compounds, based on the paramagnetic 1H NMR property. The similarity in the paramagnetic 1H NMR spectra of cofacially bridged vs monomeric systems also supports the absence of metal-metal bonding in the DPB systems.

These paramagnetic compounds were investigated to see if the temperature dependence of their proton resonances in toluene- d_8 obeys the Curie law.^{17,19} With use of variable-temperature NMR, significant chemical shift changes were observed for the proton signals of the axial ligands and of the ring periphery groups from -75 to 82 °C. Selected resonances giving rise to the largest chemical shift changes in $Ru_2(p-C_6H_4CH_3)_2DPB$ and $Os_2(CH_3)_2DPB$ are shown in Figure 3 and 4. Especially, large chemical shift changes for the axial aryl proton resonances in $Ru_2(p-C_6H_4CH_3)_2DPB$ (e.g., $|\Delta\delta| = 46.4$ for H_m ; $|\Delta\delta| = 34.4$ for H_o) were observed over the temperature range between -74 and 77 °C. Curie plots of these chemical shifts versus T^{-1} yield straight lines.

Because the two porphyrin rings are cofacially disposed and in close proximity, the Soret $\pi \rightarrow \pi^*$ transition and the Q-bands in the UV-vis absorption region tend to become broadened.²⁰ Unfortunately, these broad absorptions hamper the unambiguous assignment of the Q-bands of each compound described above.

The bisorganometallic diporphyrin complexes are air-sensitive except for the two ruthenium complexes with aryl ligands. The mass of the molecular ions was measured for the air-stable bisaryl ruthenium diporphyrins: $Ru_2(p-C_6H_4CH_3)_2DPB$, $m/e = 1486$; $Ru_2(C_6H_3(CF_3)_2)_2DPB$, $m/e = 1729$. The observed molecular ions imply that only one axial ligand per metal exists, supporting the suggested stoichiometry.

In contrast to the air-stable ruthenium complexes, osmium analogs containing axial aryl groups are air-oxidized within minutes, being cleanly converted to μ -oxo-bisarylosmium(IV) complexes. These oxidized diamagnetic compounds were identified by 1H NMR, showing that the two porphyrin rings are equivalent. The presence of an oxo rather than a superoxo bridging group was determined from the mass spectra of the oxidized osmium complexes: $Os_2(O)(p-C_6H_4CH_3)_2DPB$, $m/e = 1680$;

(13) (a) Collman, J. P.; Kim, K.; Garner, J. M. *J. Chem. Soc., Chem. Commun.* **1986**, 1711-1713. (b) Collman, J. P.; Garner, J. M. *J. Am. Chem. Soc.* **1990**, *112*, 166-173.

(14) Collman, J. P.; Prodollet, J. W.; Leidner, C. R. *J. Am. Chem. Soc.* **1986**, *108*, 2916-2921.

(15) (a) Cotton, F. A.; Curtis, N. F.; Harris, C. B.; Johnson, B. F. G.; Lippard, S. J.; Mague, J. T.; Robinson, W. R.; Wood, J. S. *Science* **1964**, *145*, 1305-1307. (b) Cotton, F. A. *Inorg. Chem.* **1965**, *4*, 334-336. (c) Cotton, F. A.; Walton, R. A. *Multiple Bonds Between Metal Atoms*; Wiley: New York, 1982; Chapter 1.

(16) Venburg, G. D. Ph.D. Thesis, Stanford University, 1990.

(17) La Mar, G. N.; Walker (Jensen), F. A. *The Porphyrins*; Dolphin, D., Ed.; Academic Press: New York, 1978; Vol. IV, Chapter 2, pp 61-157.

(18) In the $M_2(CH_3)_2DPB$ ($M = Ru, Os$) systems, the axial methyl proton signals are not detectable because of extreme line broadening. This broadening also has been observed for $M(CH_3)(OEP)$.¹⁶

(19) Swift, T. J. *NMR of Paramagnetic Molecules*; La Mar, G. N., Horrocks, W. D., Jr., Holm, R. H., Eds.; Academic Press: New York, 1973; Chapter 2.

(20) (a) Chang, C. K. *J. Heterocycl. Chem.* **1977**, *14*, 1285-1288. (b) Guillard, R.; Lopez, M. A.; Tabard, A.; Richard, P.; Lecomte, C.; Brandes, S.; Hutchison, J. E.; Collman, J. P. *J. Am. Chem. Soc.* **1992**, *114*, 9877-9889.

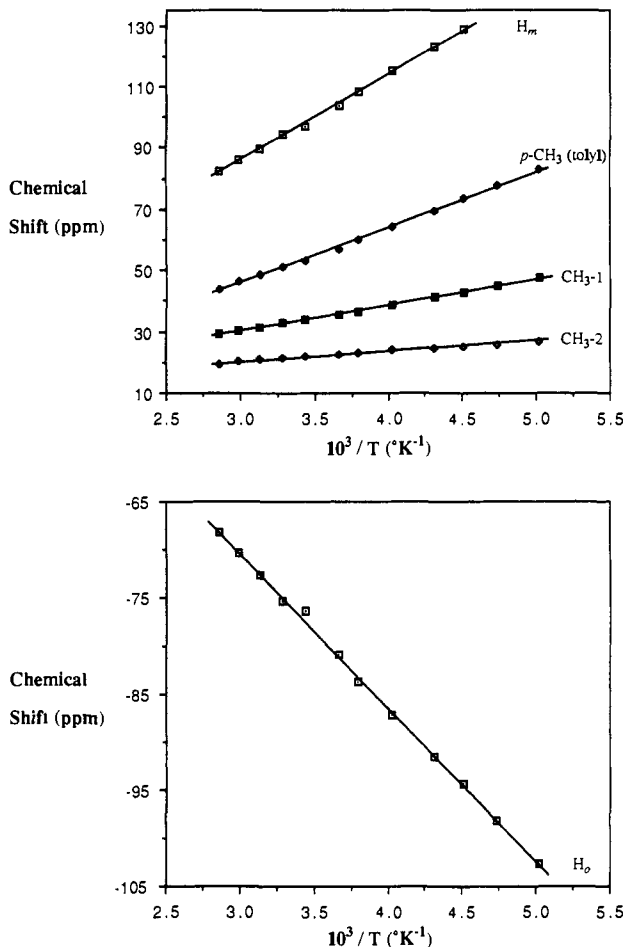


Figure 3. Curie plot for selected resonances of $\text{Ru}_2(p\text{-C}_6\text{H}_4\text{CH}_3)_2\text{DPB}$ in toluene- d_8 between -74 and 77 °C (for signal assignments, see Table IV).

$\text{Os}_2(\text{O})(\text{C}_6\text{H}_3(\text{CF}_3)_2)_2\text{DPB}$, $m/e = 1924$. Data from both ^1H NMR and mass spectrometry require that the bridged oxo ligand is inside the DPB frame and the axially ligated aryl groups reside outside. The oxidation of the osmium complexes probably occurs because third-row transition metals, with their extended 5d orbitals, are more easily oxidized than second-row transition metals.

Apparently, the reactivity toward O_2 is also influenced by a subtle electronic effect of axial ligands; upon exposure to air, methyl-coordinated ruthenium and osmium complexes do not undergo the same reactions toward oxidation as the aryl-substituted complexes. Exposure of $\text{M}_2(\text{CH}_3)_2\text{DPB}$ ($\text{M} = \text{Ru}, \text{Os}$) to air results in several poorly characterized diamagnetic species which exhibit several proton resonances of axial methyl groups upfield (-8 to -9 ppm).

Chemical Reduction of $\text{M}_2\text{R}_2\text{DPB}$. Potassium naphthalenide, $\text{K}^+\text{C}_{10}\text{H}_8^-$, was used because it is a very powerful reducing agent ($E_{1/2} = 3.19$ V vs $\text{FeCp}_2^{+/0}$)²¹ and its oxidized product, naphthalene, can be easily removed by sublimation. The solutions of $\text{M}_2\text{R}_2\text{DPB}$ ($\text{M} = \text{Ru}, \text{Os}$; $\text{R} = \text{CH}_3, 3,5\text{-(CF}_3)_2\text{C}_6\text{H}_3$) treated with potassium naphthalenide in THF yield the reduced $[\text{M}_2^{\text{II/II}}\text{R}_2\text{DPB}]^{2-}$ species (eq 1). Reduction with less than 2 equiv of the reductant results in a mixture of $[\text{M}_2^{\text{III/II}}\text{R}_2\text{DPB}]^-$ and $[\text{M}_2^{\text{II/II}}\text{R}_2\text{DPB}]^{2-}$.

Using ^1H NMR, we were able to observe these compounds in all of their reduced and neutral forms. While the neutral $\text{M}_2^{\text{III/III}}\text{R}_2\text{DPB}$ complexes and the intermediate reduction products, $[\text{M}_2^{\text{III/II}}\text{R}_2\text{DPB}]^-$, display paramagnetic, contact-shifted ^1H NMR spectra, the fully reduced $[\text{M}_2^{\text{II/II}}\text{R}_2\text{DPB}]^{2-}$ species show

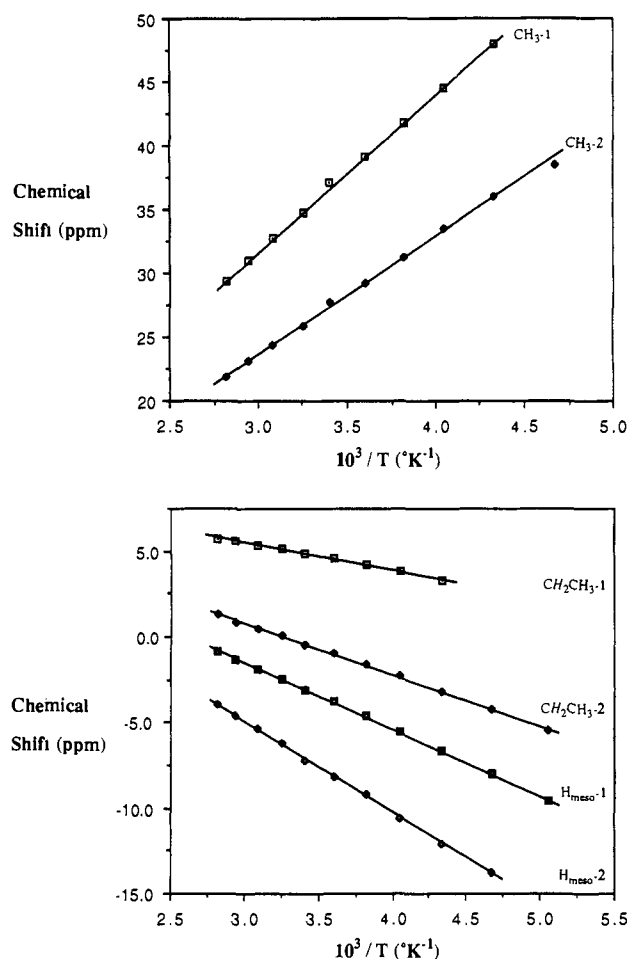
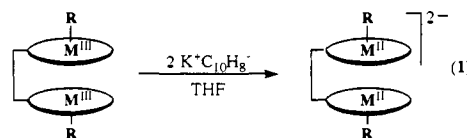


Figure 4. Curie plot for selected resonances of $\text{Os}_2(\text{CH}_3)_2\text{DPB}$ in toluene- d_8 between -75 and 82 °C (for signal assignments, see Table IV).



well-resolved, diamagnetic spectra. The symmetry shown in the ^1H NMR spectra indicates that all the complexes have C_2 symmetry, that is, the two porphyrin rings and axial ligands are equivalent.

The identity of each singly reduced monoanionic species was confirmed by comparing its spectrum with that of the same compound prepared independently. Samples of the mixed-valence monoanion $[\text{M}_2^{\text{III/II}}\text{R}_2\text{DPB}]^-$ were prepared in two ways: (a) by mixing equal amounts of the dianion with the neutral, and (b) by treating the dianion with an acid with $\text{pK}_a > 9$, *vide infra*. Solutions of the monoanion prepared by both methods show identical ^1H NMR spectra. The ^1H NMR spectra of $[\text{M}_2^{\text{III/II}}\text{R}_2\text{DPB}]^-$ also show that the two porphyrin rings are equivalent, indicating fast electron transfer between two metal centers on the NMR time scale and a fast electron-relaxation time. The $[\text{M}_2^{\text{III/II}}\text{R}_2\text{DPB}]^-$ proton signals appear in a range between the chemical shifts of the diamagnetic dianions and those of the paramagnetic neutral complexes. Similar trends in chemical shifts were reported in the NMR spectra of neutral and oxidized products of $\text{M}_2(\text{OEP})_2$ ($\text{M} = \text{Ru}, \text{Os}$) which are isoelectronic with reduced and neutral $\text{M}_2\text{R}_2\text{DPB}$ series.¹⁴ In that study, intermediate monocations, $[\text{M}_2^{\text{III/II}}(\text{OEP})_2]^+$, show chemical shifts of proton resonances in between those of paramagnetic $[\text{M}^{\text{II}}(\text{OEP})]_2$ and diamagnetic $[\text{M}^{\text{III}}(\text{OEP})]_2^{2+}$.

Electrochemistry of $\text{M}_2\text{R}_2\text{DPB}$. Cyclic voltammetry was performed on all $\text{M}_2\text{R}_2\text{DPB}$ species in THF. Clean waves were observed in the cyclic voltammograms of all six compounds studied

(21) Perichon, J. *Encyclopedia of Electrochemistry of the Elements*; Bard, A. J., Lund, H., Eds.; Marcel Dekker: New York, 1978; Vol. 11, Chapter 1, p 72.

Table I. Reduction Potentials of Cofacial Bisorganometallic Diporphyrin Complexes

M	R	$E_{1/2}$ (V) vs $\text{FeCp}_2^{+/0}$ ^a		estimated $E_{1/2}$ (V) vs NHE ^{b,c}	
		$\text{M}_2(\text{III})(\text{III})/\text{M}_2(\text{III})(\text{II})$	$\text{M}_2(\text{III})(\text{II})/\text{M}_2(\text{II})(\text{II})$	$\text{M}_2(\text{III})(\text{III})/\text{M}_2(\text{III})(\text{II})$	$\text{M}_2(\text{III})(\text{II})/\text{M}_2(\text{II})(\text{II})$
Ru		-0.94	-1.38	-0.39	-0.83
		-1.26	-1.45	-0.71	-0.90
	-CH ₃	-1.38	-1.72	-0.83	-1.17
Os		-1.18	-1.58	-0.63	-1.03
		-1.47	-1.69	-0.92	-1.14
	-CH ₃	-1.55	-1.97	-1.00	-1.42

^a The cyclic voltammograms of the complexes were obtained in freshly distilled THF containing 0.2 M tetra-*n*-butylammonium hexafluorophosphate. The data were recorded at a scan rate of 100 mV/s. ^b $\text{FeCp}_2^{+/0} = +0.31$ V vs SCE; SCE = +0.24 V vs NHE. ^c The measurements of the half-wave potentials were performed in THF. The reference values of FeCp_2 vs SCE and SCE vs NHE were taken from the values measured in CH_3CN and H_2O , respectively.^{21,22}

($\Delta E_p = 69 \pm 2$ mV). The results are shown in Table I. Any paramagnetic, NMR invisible impurities should have been revealed by these electrochemical experiments. THF was chosen as a solvent for electrochemical analysis because it has a wide reduction window. However, potential conversions between standard references (NHE, SCE) and substrates are approximations²²⁻²⁴ because data for quantitative comparison of reference potentials in THF are not available.

Four waves were usually observed for each of the cofacial bisorganometallic diporphyrin complexes within the solvent breakdown limits. The identity of each wave (an oxidation or a reduction) was determined by comparing the voltammograms of the DPB complexes with the cyclic voltammogram of monomeric metalloporphyrins such as $\text{Os}(\text{OEP})(\text{CH}_3)$. We found the latter to display only two waves: a one-electron oxidation ($E_{1/2} = -0.35$ V vs FeCp_2) and a metal-based one-electron reduction²⁵ ($E_{1/2} = -1.59$ V vs FeCp_2). On the basis of this information and the chemical redox properties of the cofacial bisorganometallic diporphyrins described above, the two reduction waves are assigned to $\text{M}_2(\text{III})(\text{III})/\text{M}_2(\text{III})(\text{II})$ and $\text{M}_2(\text{III})(\text{II})/\text{M}_2(\text{II})(\text{II})$ couples, respectively. Definitive assignment of the two oxidation waves has not been attempted because it is irrelevant to this study. We suppose these are $\text{M}_2(\text{III})(\text{III})/(\text{III})(\text{IV})$ and $\text{M}_2(\text{III})(\text{IV})/(\text{IV})(\text{IV})$. The oxidation and the reduction waves are all reversible, and successive scans do not diminish their peak currents. Thus, on the time scale of these experiments, we observe no chemical reactions following electron transfer.

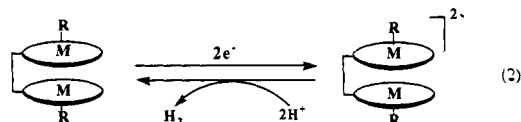
Hydrogen Evolving Reactions of $[\text{M}_2\text{R}_2\text{DPB}]^{2-}$. Addition of acids, with suitable (*vide infra*) pK_a values, to the anions of $\text{M}_2\text{R}_2\text{DPB}$ species in THF led to H_2 evolution with concomitant oxidation of the complexes to the neutral species as observed by ^1H NMR (eq 2). Dihydrogen formation was analyzed by GC;

(22) Bard, A. J.; Faulkner, L. R. *Electrochemical Methods: Fundamentals and Applications*; John Wiley and Sons: New York, 1980.

(23) Anson, F. C.; Collins, T. J.; Richmond, T. G.; Sanarsiero, B. D.; Toth, J. E.; Treco, B. G. R. *J. Am. Chem. Soc.* **1987**, *109*, 2974-2979.

(24) Sawyer, D. T.; Roberts, J. L., Jr. *Experimental Electrochemistry for Chemists*; John Wiley & Sons: New York, 1974.

(25) It was also reported that redox reactions in many organometallic porphyrins are metal based. As a general review, see: Guillard, R.; Kadish, K. M. *Chem. Rev.* **1988**, *88*, 1121-1146.



approximately 60% of the stoichiometric H_2 (vs the amount of cofacial bisorganometallic diporphyrin complexes employed) was detected. Because quantitative proton reduction to H_2 was not observed, side reactions which consume hydrides produced by protonation at the metal center must be occurring.²⁶

Addition of a certain acid may or may not result in the oxidation of the anions of $\text{M}_2\text{R}_2\text{DPB}$, depending upon the basicity of these anions. When acids in a medium pK_a range are used, the dianions of $\text{M}_2\text{R}_2\text{DPB}$ are converted solely to their monoanions. Successive addition of a stronger acid to the monoanions leads to the complete oxidation of the reduced cofacial complexes. The aqueous pK_a values of the acids required to oxidize completely the dianion to the neutral $\text{M}_2\text{R}_2\text{DPB}$ are listed in Table II. Note that the pK_a values of the acids which completely oxidize the dianions to the neutrals parallel the reduction potentials of the dianions (Table I). That is, the complexes with the lowest reduction potentials require the weakest acids for their oxidation. This is the expected result.

In the $\text{M}_2(p\text{-C}_6\text{H}_4\text{CH}_3)_2\text{DPB}$ series, two-electron reduction does not give distinct diamagnetic ^1H NMR spectra, prohibiting their pK_a measurements. However, on the basis of their reduction potentials in comparison with those of $\text{M}_2(\text{C}_6\text{H}_3(\text{CF}_3)_2)_2\text{DPB}$ and $\text{M}_2(\text{CH}_3)_2\text{DPB}$, it can be predicted that the pK_a values required to completely discharge $\text{M}_2(p\text{-C}_6\text{H}_4\text{CH}_3)_2\text{DPB}$ are probably between those of $\text{M}_2(\text{C}_6\text{H}_3(\text{CF}_3)_2)_2\text{DPB}$ and $\text{M}_2(\text{CH}_3)_2\text{DPB}$.

Catalytic Proton Reduction Activity with Mercury-Pool Electrodes. We had hoped to use sacrificial reductants to perform catalytic proton reduction with these complexes. Certain criteria should be considered when choosing reducing agents for proton reduction. (1) Ideal reducing agents should have reduction potentials low enough to reduce the catalysts, (2) but they should have high overpotentials for proton reduction so that only the $\text{M}_2\text{R}_2\text{DPB}$ catalysts (not the sacrificial electron donor) can reduce protons. (3) Finally, reducing agents should be able to supply electrons continuously and efficiently to the catalysts. A number of reducing reagents were tried without success: $\text{K}^+\text{C}_{10}\text{H}_8^-$, Na/Hg, Zn/Hg, Al/Hg, Mg/Hg, and Ca/Hg amalgams (note that Hg has a high proton reduction overpotential),²⁷ SmI_2 and cobaltocene (CoCp_2). Consequently, we decided to use Hg-pool electrodes to investigate catalytic proton reduction by $\text{M}_2\text{R}_2\text{DPB}$.

In an inert atmosphere box, the mercury-pool electrode^{27,5a} in contact with metalloporphyrin and acid solutions was potentiostated to a certain potential (vs Ag wire). The voltage applied was chosen such that measurable quantities of H_2 were produced. Attempts to reference these reduction potentials versus either ferrocene or cobaltocene at the end of each experiment failed because no reversible redox wave was observed on the Hg-pool electrode under the conditions of the catalytic experiments. The amount of H_2 evolved from the electrolyses at each fixed potential was assayed by injecting gas samples taken from the sealed headspace above the working electrode solution into a GC. Stirring was crucial for supplying electrons continuously to the catalysts; otherwise the H_2 evolution was quite slow.

A very negative potential (-1.8 V vs Ag) was needed for a complex such as $\text{Os}_2(\text{CH}_3)_2\text{DPB}$ (which has the lowest reduction potential in Table I) to act as a catalyst for proton reduction. In contrast, a less negative potential (by 600 mV) was needed to

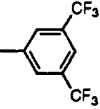
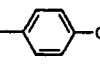
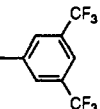
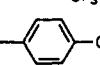
(26) Apparently by ^1H NMR, only the reaction in eq 2 was observed and thus could be analyzed. Some solvents or other substrates present in the solution might have been reduced by the hydrides; as yet, those other substrates have not been detected and identified.

(27) Ruetschi, P. *The Encyclopedia of Electrochemistry*, Hampel, C. A., Ed.; Reinhold Publishing: New York, 1964; pp 869-875.

Table II. Acids and pK_a Values Required To Oxidize the Dianions Completely

dianion	acid employed	pK_a (in H ₂ O) of acid ³⁵
[Ru ₂ ^{II/II} (C ₆ H ₃ (CF ₃) ₂) ₂ DPB] ²⁻	trifluoroacetic acid	0.2
[Os ₂ ^{II/II} (C ₆ H ₃ (CF ₃) ₂) ₂ DPB] ²⁻	<i>o</i> -nitrobenzoic acid	2.2
[Ru ₂ ^{II/II} (CH ₃) ₂ DPB] ²⁻	<i>p</i> -nitrophenol	7.1
[Os ₂ ^{II/II} (CH ₃) ₂ DPB] ²⁻	<i>o</i> -chlorophenol	8.5

Table III. Catalytic Proton Reduction on Hg-Pool Electrodes

M	R	holding potential (V vs Ag)	catalytic turnover (over 20 min) ^{a,b}	acids employed
Ru		-1.2	1.6	CF ₃ COOH
		-1.7	1.7	C ₆ H ₅ COOH
	-CH ₃	-1.7	2.0	CF ₃ COOH C ₆ H ₅ COOH
Os		-1.6	2.2	C ₆ H ₅ COOH
		-1.8	2.3	C ₆ H ₅ COOH
	-CH ₃	-1.8	3.3	C ₆ H ₅ COOH

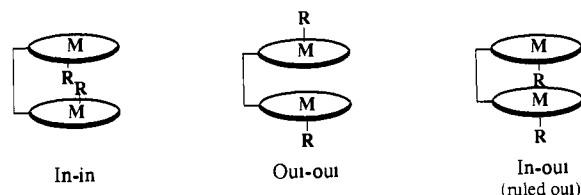
^a The amount of H₂ evolved from electrolysis was detected by GC.

^b When more negative potentials than the listed ones were applied or when longer electrolysis was performed, higher catalytic turnovers (up to 5.5) resulted.

observe proton reduction catalysis with Ru₂(C₆H₃(CF₃)₂)₂DPB. Applying comparatively less negative potentials (vs Ag) than the reduction potential of the catalyst at a Pt electrode (vs FeCp₂ as referenced vs Ag) does not result in appreciable H₂ evolution. This indicates that reduction of the cofacial metalloporphyrin species is pre-requisite for catalytic proton reduction. The applications of a constant potential sufficient for catalyst reduction and the use of suitable proton sources resulted in catalytic production of H₂ which was detected by GC after the 20-min electrolyses. In the presence of the catalyst and a suitable acid, between 1.6 and 5.5 mol of H₂ were produced per mol of catalyst over a 20-min period (Table III).

Recall that our pK_a studies demonstrate that the basicity of the complexes is related to their reduction potentials. For instance, Ru₂(C₆H₃(CF₃)₂)₂DPB and Ru₂(*p*-C₆H₄CH₃)₂DPB which display the least negative reduction potentials do not produce a significant amount of H₂ with benzoic acid as the oxidant. Thus, when these catalysts were employed, a stronger acid such as trifluoroacetic acid had to be used for proton reduction at the controlled potential. Conversely, those catalysts which are easier to oxidize (i.e., have more negative reduction potentials) display rapid H₂ formation with weaker acids such as benzoic acid.

Several control experiments were performed to confirm that the proton reduction is indeed catalyzed by these cofacial bioorganometallic diporphyrin complexes. In the absence of acids and catalysts, electrolysis of the supporting electrolyte solution (TBAPF₆ in THF) gave an insignificant amount of H₂. Electrolysis of proton sources (benzoic acid and trifluoroacetic acid) without a catalyst was also examined. Insignificant amounts of H₂ were produced even at a constant potential of -2.0 V (vs Ag), which is much more negative than the potentials used for the electrolyses involving a combination of the catalysts and acids. To investigate whether protons are actually reduced at the metal center, pyridine was added to the electrocatalytic system. Pyridine should bind tightly to the metal centers inside of DPB,²⁸ blocking the catalytic coordination site. Proton reduction was inhibited

**Figure 5.** Possible regioisomers in cofacial bisorganometallic diporphyrin complexes.

by a trace of pyridine. This control experiment implies that proton reduction, in fact, occurs at the metal center and pyridine can effectively inhibit this reaction by blocking the site for proton coordination.

The catalysts decompose over periods of about 5 h under several extensive electrolyses in the presence of acids. The osmium complexes are more robust than the ruthenium analogs, and complexes with axial methyl groups are more stable than those with axial aryl groups. These decompositions were detected by monitoring the disappearance of the first oxidation wave of each catalyst, which is the only well-resolved reversible wave in the cyclic voltammogram at Hg-pool working electrodes.

Discussion

¹H NMR Properties of M₂R₂DPB and of Corresponding Anions. ¹H NMR spectroscopy is indispensable in identifying bisorganometallic diporphyrins and in investigating their magnetic properties. The symmetry indicated by the ¹H NMR spectra of these cofacial complexes reveals that the two porphyrin rings are equivalent. That is, their ¹H NMR spectra demonstrate C_{2v} symmetry, featuring only one set of axial ligand arrangements. From these ¹H NMR characteristics, two regioisomers can be considered: in-in or out-out isomers (Figure 5). These may be distinguished by comparison to the monomeric analogs M(R)-(OEP). We found that axial ligand proton resonances in the cofacial complexes are similar to those observed in the monomeric analogs. This evidence supports the out-out isomer formulation because the axial ligands on the out-out isomers should experience ring current effects from the porphyrin similar to those from the monomeric systems. Axial ligands on in-in isomers would experience additional shielding caused by two aromatic porphyrin rings, shifting proton resonances of the inner axial ligands upfield relative to M(R)(OEP). The cofacial bisorganometallic diporphyrin complexes would then show ¹H NMR spectra different from the monomeric compounds. In-in isomer formation is probably prohibited because a metal-metal triple bond between the two oxidized metals within DPB may block a nucleophile from approaching inside (see Figure 1). Furthermore, the geometry of the cofacial diporphyrins prevents side reactions such as double alkylation or arylation from occurring because the steric effect from the cofacial dimetalloporphyrin prevents another alkyl or aryl group from attacking inside the DPB pocket. Thus, the cofacial diporphyrin yields only one specific regioisomer which we believe has both axial ligands outside.

The observed proton chemical shift dependence on temperature reflects the paramagnetism associated with the unpaired electron in each d⁵ M(III) center (see Figures 3 and 4). The unpaired electrons on the metal ion can be delocalized onto the porphyrin or the axial ligands via overlap of a ligand molecular orbital and a metal d orbital. The spin transfer occurs via σ bonding and/or π bonding. In porphyrin complexes, the d_{xz} and d_{yz} orbitals of the metal are capable of π bonding, and in 4-fold symmetry (D_{4h}) these two orbitals have e symmetry. Since Ru(III) and Os(III) have an unpaired spin in the d_{xz} or d_{yz} orbital, this π spin density can be transferred from metal (d_{xz} or d_{yz}) to the porphyrin ligand (4e π^*) through back-bonding. This back-bonding results in downfield contact shifts for CH₃ or CH₂ groups on the β -pyrrolic

(28) Pyridine coordination inside as well as outside of M₂DPB was previously reported by our group. See ref 13.

carbon according to the predicted electron distribution of the porphyrin orbitals.¹⁷ The exceptional upfield chemical shift of one diastereotopic, β -pyrrolic methylene proton signal in M_2R_2 -DPB is probably due to the additional ring current effect from the other porphyrin ring on the rotationally hindered methylene proton facing inside of DPB. The chemical shifts of *p*-tolyl groups in $Ru_2(p-C_6H_4CH_3)_2DPB$ exhibit alternating signs among H_m , H_o , and *p*-CH₃ of the tolyl group. This illustrates that the unpaired π spin density is also delocalized onto the axial ligand.¹⁷ These NMR characteristics, therefore, confirm π spin transfer from metal orbitals (d_{xz} or d_{yz}) to both axial ligand and porphyrin orbitals.

As mentioned earlier, the fully reduced dianions, $[M_2-(CH_3)_2DPB]^{2-}$ ($M = Ru, Os$), display diamagnetic ¹H NMR spectra. These reduced species exhibit axial methyl proton signals around -9.8 ($M = Ru$) and -12 ppm ($M = Os$) while axial methyl group resonances of neutral paramagnetic $M_2(CH_3)_2DPB$ and of their monoanions are not observed in the ¹H NMR spectra due to extreme line broadening. The chemical shifts of the axial methyl proton resonances in these cofacial $[M_2^{II/III}(CH_3)_2DPB]^{2-}$ systems are quite comparable to those values at -9.08 ($M = Ru$)²⁹ and -11.76 ppm ($M = Os$)³⁰ for the monomeric $[M^{II}(CH_3)OEP]^-$ systems. This further supports our formulation of the out-out regioisomer.

Reduction of the $M_2(CH_3)_2DPB$ complexes with 2 equiv of $K^+C_{10}H_8^-$ under a N_2 atmosphere sometimes yields two different reduced species featuring two separate upfield methyl signals ($Ru^{II}-CH_3$ at -9.2 and -10.3 ppm; $Os^{II}-CH_3$ at -11.6 and -12.5 ppm) with two corresponding sets of porphyrin proton resonances. These independent sets display different intensities, each showing C_{2v} symmetry. The nature of these subtle changes in the ¹H NMR spectra is not clear; among the possible explanations is a change in the nature of axial ligands weakly bound within the diporphyrin cavity. Such ligands include THF (the solvent) or even N_2 . Dinitrogen was reported to compete as a ligand with THF in $Ru(Por)$ systems¹⁶ and to be present as a bridging ligand in a similar cofacial complex, $\mu-N_2-Ru_2L^*DPB$ ($L^* = 1$ -*tert*-butyl-5-phenylimidazole).³¹ We demonstrated by GC analysis after the introduction of pyridine that N_2 is not evolved; thus N_2 is not a competing ligand. THF is probably the inhibiting ligand.

Synthetic Control of the Catalyst Reduction Potential. We have tried to develop a catalytic proton reduction system using cofacial metalloporphyrins and to control the overpotential for proton reduction by systematically varying central metals and axial ligands. We have achieved our synthetic goal by preparing a series of six cofacial porphyrin complexes of ruthenium and osmium, each fitted with a series of three external axial ligands. Their reduction potentials have been measured and the intermediate reduction products characterized (especially the diamagnetic $M_2(II)(II)$ dimer dianions by ¹H NMR). The pK_a values of the acids required to oxidize the reduced form of the catalysts have been shown to be consistent with the nature of the axial ligand and the central metal. Weak acids with high pK_a values cannot protonate the reduced metalloporphyrin catalysts which have the least negative reduction potentials, and thus H_2 evolution was not observed under those circumstances. Conversely, those catalysts which have more negative reduction potentials display rapid proton reduction with weaker acids such as *o*-chlorophenol when supplied with electrons.

These complexes demonstrated modest catalysis of proton reduction at mercury electrodes. Reductive formation of H_2 is

(29) Collman, J. P.; Ha, Y. Unpublished results. The reduction of monomeric $Ru(CH_3)OEP$ yields the corresponding monoanion: ¹H NMR (THF- d_8 , ppm): H_{meso} 8.08 (s, 4H); CH_2CH_3 3.42 (m, 16H); CH_2CH_3 1.63 (t, 24H); $RuCH_3$ -9.08 (s, 3H).

(30) Collman, J. P.; Ha, Y. Unpublished results. The reduction of monomeric $Os(CH_3)OEP$ yields the corresponding monoanion: ¹H NMR (THF- d_8 , ppm): H_{meso} 6.98 (s, 4H); CH_2CH_3 3.43 (q, 16H); CH_2CH_3 1.59 (t, 24H); $OsCH_3$ -11.76 (s, 3H).

(31) (a) Collman, J. P.; Hutchison, J. E.; Lopez, M.-A.; Guillard, R.; Reed, R. A. *J. Am. Chem. Soc.* **1991**, *113*, 2794–2796. (b) Collman, J. P.; Hutchison, J. E.; Lopez, M.-A.; Guillard, R. *J. Am. Chem. Soc.* **1992**, *114*, 8066–8073.

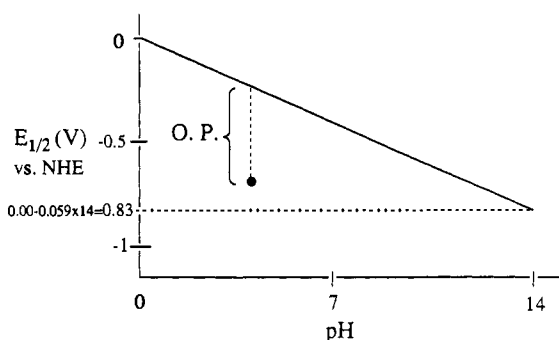


Figure 6. Plot of the Nernst equation for proton reduction.

found to be rather slow (turnover numbers 1.6–5.5 per 20 min) in each electrocatalysis with these complexes. One possible explanation which has been discussed above is that THF solvent molecules may inhibit catalytic proton reduction by blocking the inside of DPB. Another possible reason for the slow proton reduction and H_2 evolution rate is that the outer axial ligands may pull out the metal centers from the porphyrin plane significantly, making the protonation on the metal centers or dihydrogen elimination difficult.

The main purpose in applying cofacial bisorganometallic diporphyrin complexes to proton reduction is to facilitate dinuclear H_2 elimination by taking advantage of these cofacially oriented complexes. The electrochemistry on a Hg-pool electrode and ¹H NMR investigation of mononuclear $Os(CH_3)(OEP)$ in the presence of a proton source show that the mononuclear system displays a smaller catalytic current and is less robust than its cofacial analog. This implies that proton reduction can indeed take advantage of the cofacial orientation of DPB, but catalysis is not as rapid as we expected—perhaps due to solvent inhibition in the restricted catalyst cavity.

As expected, the more electropositive complexes reduce protons at more positive potentials. However, the absolute potential at which these complexes achieve catalytic proton reduction is not the feature of prime importance. Rather, it is the *overpotential* which is paramount. The plot of the Nernst equation in Figure 6 demonstrates that the thermodynamic potential, $E_{1/2}$, for proton reduction is dependent on pH. Thus, if proton reduction is achieved at a given pH and potential shown by the point in Figure 6, the overpotential (OP) is measured as the vertical distance between the point and the Nernstian line. (Note that above the solid line, proton reduction catalysis is prohibited.)

Unfortunately, we were unable to measure accurately the overpotentials for the metalloporphyrin systems discussed above due to the lack of pH data in THF and the uncertainty of the catalyst potentials relative to NHE. However, useful information can still be extracted from these experiments if we remind ourselves of our initial goal. We had hoped that by making electrocatalysts with reduction potentials less extreme, or less negative, we would also affect the overpotential. If the overpotential increased as we make more electropositive catalysts, our modifications would be unproductive.

Thus, it is instructive to plot the $E_{1/2}$ of the catalyst (i.e. the potential required to generate the active form of the catalyst) versus the pH required to produce hydrogen from that catalyst (Figure 7). The bold line represents the catalyst modification we desired.

Figure 8 plots our data for the $E_{1/2}$ of the catalyst versus the aqueous pK_a of the acid required to yield H_2 from that catalyst. The absolute values on the plot are meaningless because we do not accurately know the pH in THF. However, the relative pK_a values should not change and it is the relative values that determine the slope. Note that the slope of the above plot, -0.06 V/ pK_a unit, is identical, within experimental error, to the Nernstian slope (0.059 V/ pK_a unit). This indicates that nothing was gained by the catalyst modifications. Changing the central metal within

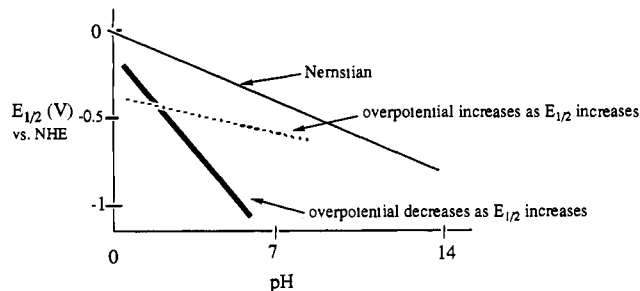


Figure 7. Several scenarios for catalytic potential vs pH for proton reduction.

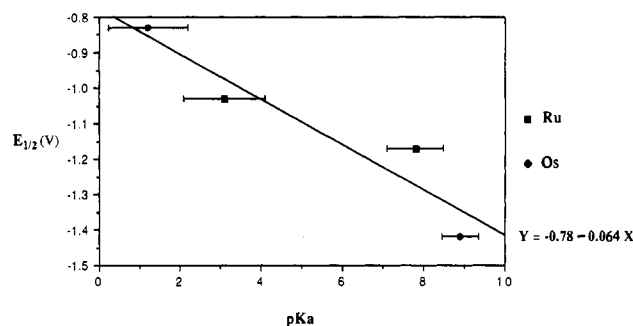


Figure 8. Actual plot of the reduction potential vs the pK_a of the catalyst systems. The left-hand sides of the error bars indicate the pK_a of acid which results in complete oxidation of the catalysts. The right-hand sides of the error bars indicate the pK_a of acid which results in partial oxidation of the catalysts.

a single column and/or modification of the axial ligand did not result in significant reductions of the overpotential. The limited data that we were able to obtain indicate that *modification of the reduction potentials of a closely related set of catalysts results in insignificant changes in the overpotential for proton reduction*. Perhaps switching the central metal for one in another column would effect the desired change.

Switching the central metal to cobalt is attractive because cobalt porphyrins have demonstrated electrochemical proton reduction catalysis.⁵ However, the synthesis of the cofacial dicobalt analogues has suffered from poor regiochemical control. A nucleophile such as a carbanion equivalent can attack the cobalt center from the inside of DPB perhaps because Co contains 3d electrons and does not form metal-metal bonds. Another drawback which should be considered is the intolerance of organocobalt porphyrin complexes to the electrocatalytic conditions;³² Co-C bonds may be cleaved in very acidic media.

Mechanism. Several steps in the catalytic cycle of proton reduction already have been established by ¹H NMR. Two plausible pathways are suggested for proton reduction and concomitant H₂ evolution by M₂R₂DPB complexes, based on these observations.

A mechanism requiring both metal centers to be protonated is shown in Figure 9, featuring dihydride intermediates (I). In this mechanism, dihydrogen is eliminated (Ic) from two metal hydrides (I).

Alternatively, this proton reduction process can be described as a unimetallic process in which successive protonation (IIb and IIc) and dihydrogen elimination (IId) occur at one metal center accompanied by electron transfer from the metal anion on the other side (Figure 10). In the latter mechanism, the second protonation thus occurs at the metal hydride site rather than the other basic metal center (IIc), and thus, a dihydrogen complex (II) is supposed to form at a single metal center.

There are precedents for both a dihydride and a dihydrogen complex acting as a possible intermediate in the H₂ evolution process. The mechanism of H₂ evolution involving diprotonated

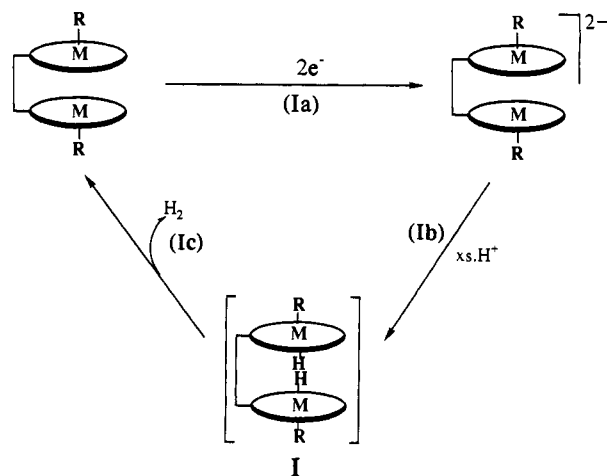


Figure 9. A mechanism involving a dihydride intermediate (I).

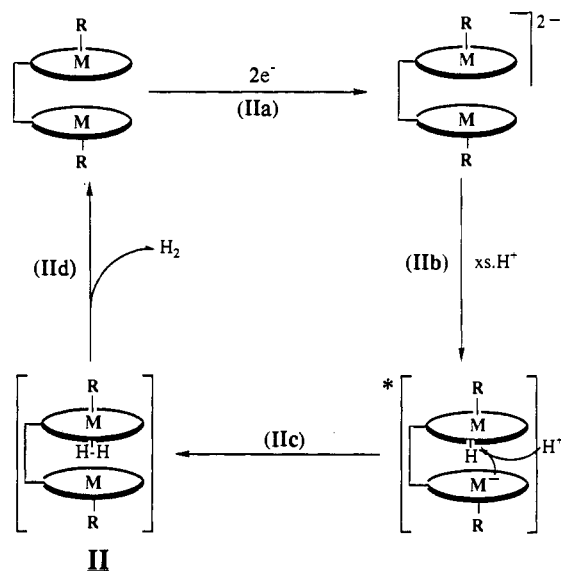


Figure 10. A mechanism involving a dihydrogen complex intermediate (II). The step for the second proton transfer and electron transfer (indicated with an asterisk) is actually two steps and is not concerted as it is indicated.

dimetal centers was suggested in bridged bismetallocenes.⁷ Additional support for a bimolecular mechanism requiring two protonated metal centers was reported recently by our group based on the result of double potential step chronoamperometry.¹² In that study, H₂ elimination was proposed to occur bimolecularly via two transient neutral metalloporphyrin hydrides resulting from the oxidation of metalloporphyrin hydride anions.

By contrast, the involvement of only a single metal center for H₂ elimination was proposed by Norton et al.⁹ kinetically protonation on a metal hydride might be more facile than on the other metal center so that the second protonation could occur on the metal hydride site instead of at the other metal. The unimetallic process evolving H₂ from the dihydrogen complex is ubiquitous since many examples of dihydrogen complex formation from the protonation of transition metal hydride systems have been reported.³³

In studies of H₂ evolution from cobalt porphyrins, the reaction was thought to proceed by two parallel pathways such as those described above.⁵ In the systems studied herein, it cannot be determined whether one of the above processes is dominant or even exclusive. Attempts to isolate hydridic intermediates by protonation at low temperatures failed. At this time, we consider

(32) Shi, S.; Bakac, A.; Espenson, J. H. *Inorg. Chem.* **1991**, *30*, 3410-3414.

(33) For general reviews, see: (a) Kubas, G. J. *Acc. Chem. Res.* **1988**, *21*, 120-128. (b) Crabtree, R. H.; Hamilton, D. G. *Adv. Organomet. Chem.* **1988**, *28*, 299-338.

Table IV. ^1H NMR Data for $\text{M}_2\text{R}_2\text{DPB}$ (C_6D_6 , 400 MHz, ppm 18 °C)

compds	H_{meso} (2H, 4H)	$-\text{CH}_3$'s (12H each)	$-\text{CH}_2\text{CH}_3$ (4H each)	$-\text{CH}_2\text{CH}_3$ (12H each)	R (axial ligands)
$\text{Ru}_2(\text{CH}_3)_2\text{DPB}$	1.04, 0.79	34.9, 23.5	8.87, 8.12, 6.84, 0.90	-0.85, -1.04	not observed ^b
$\text{Ru}_2(p\text{-tolyl})_2\text{DPB}$	between 8 and 2 ^a	33.9, 22.3	13.2, 11.4, 3.9, 2.1	-0.8, -1.1	97.8 (H_m , 4H), -76.5 (H_o , 4H), 53.3 ($p\text{-CH}_3$, 6H)
$\text{Ru}_2(\text{C}_6\text{H}_3(\text{CF}_3)_2)_2\text{DPB}$	0.86, 4.60	44.3, 24.0	15.1, 12.4, 12.2, 2.99	0.05, -0.31	-4.46 (H_p , 2H), -43.5 (H_o , 4H)
$\text{Os}_2(\text{CH}_3)_2\text{DPB}$	-3.17, -7.19	36.9, 27.6	6.31, 5.39, 5.15, -0.42	-0.07, -0.3	not observed ^b
$\text{Os}_2(p\text{-tolyl})_2\text{DPB}$	-6.92, -8.00	26.2, 18.2	6.42, 6.37, 2.72, -1.71	-1.21, -1.39	70.7 (H_m , 4H), -44.6 (H_o , 4H), 57.3 ($p\text{-CH}_3$, 6H)
$\text{Os}_2(\text{C}_6\text{H}_3(\text{CF}_3)_2)_2\text{DPB}$	-5.63, -3.89	32.6, 19.3	7.94, 7.22, 5.88, -0.33	-0.14, -0.39	2.36 (H_p , 2H), -32.9 (H_o , 4H)

^a Overlapped with $\text{H}_{\text{biphenylene}}$ signals. ^b Not observed due to line broadening.

that catalytic reductive H_2 elimination with cofacial bisorganometallic diporphyrin complexes can occur through both pathways.

Conclusion

Six cofacial bisorganometallic diporphyrins have been synthesized and their activity as proton reduction catalysts has been investigated. ^1H NMR has been used to keep track of the overall process stoichiometrically. The complexes synthesized in this study have displayed catalytic proton reduction activity on mercury-pool electrodes. A wide range of reduction potentials has been obtained by employing two metals (Ru and Os) and three carbon-based axial ligands with differing electronic properties. The basicity of reduced bisorganometallic diporphyrin species has been analyzed. Both the reduction potential and the basicity of these complexes reflect their intrinsic electronic properties as predicted. The effectiveness of the ligand and metal modifications with respect to the overpotential of the catalysis was analyzed and found to be insignificant (within experimental error) for modifications within a closely related series of catalysts. We conclude that to lower the overpotential for proton reduction significantly, more extreme modifications, such as changing the porphyrin ligand or changing the central metal to one from outside the Fe column, must be performed.

Experimental Section

Solvent and Reagents. All solvents used in the inert atmosphere box were purified prior to use. Toluene, benzene, hexanes, and diethyl ether were distilled from purple or blue sodium benzophenone ketyl solutions under a nitrogen atmosphere. The solvents were then transferred into the drybox in sealed flasks and sparged with nitrogen for 20–30 min to remove residual oxygen. Tetrahydrofuran from a freshly opened bottle was treated with CaH_2 overnight and was further dried by distillation from its sodium and potassium benzophenone ketyl solution. For best results, fresh THF for electrochemical experiments and for proton or water sensitive reactions was used within 1 week of distillation. Small amounts (ca. 25 mL) of freshly purified THF were vacuum transferred from sodium/potassium benzophenone ketyl solution frequently. Dichloromethane was dried by distillation from P_2O_5 under a nitrogen atmosphere and sparged with drybox atmosphere gas. Deuterated solvents were dried and degassed prior to use. Benzene- d_6 , toluene- d_8 , and tetrahydrofuran- d_8 were purified by forming their respective sodium/potassium benzophenone ketyl solutions in Schlenk flasks and vacuum transferring the solvents to other flasks. Dichloromethane- d_2 and chloroform- d_1 were passed down a basic alumina column, dried with P_2O_5 in a Schlenk flask, vacuum transferred to a clean, dry Schlenk flask, and brought into the drybox. Flash chromatographic silica gel (EM Science, Kieselgel 60H), gravity alumina (Fisher, Neutral, 80–200 mesh), and Celite for drybox use were dried and degassed under vacuum (300 °C, 10^{-2} Torr) for at least 24 h and stored in the drybox. All other commercially available reagents were used as received.

Instruments and Measurements. All manipulations of oxygen- and water-sensitive compounds were performed in a Vacuum/Atmosphere Co. nitrogen atmosphere drybox ($\text{O}_2 \leq 2$ ppm). Oxygen levels were monitored with an AO316-C trace oxygen analyzer. Oxygen and moisture sensitive materials were also handled on a vacuum line or in Schlenkware flasks equipped with E. J. Young valves and O-ring vacuum adapter fittings.

^1H NMR spectra were obtained mostly with a Nicolet NMC 300-MHz spectrometer or with a Varian XL 400-MHz instrument. A GEM 200-MHz instrument was also used to record ^1H NMR spectra. All chemical shifts are reported in units of δ (downfield from tetramethylsilane) but were measured relative to residual ^1H resonances in deuterated

Table V. UV Data for $\text{M}_2\text{R}_2\text{DPB}$ (Toluene, λ_{max} , nm)

compd	Soret	Q-bands
$\text{Ru}_2(\text{CH}_3)_2\text{DPB}$	364	469 (sh), 508
$\text{Ru}_2(p\text{-tolyl})_2\text{DPB}$	368	518
$\text{Ru}_2(\text{C}_6\text{H}_3(\text{CF}_3)_2)_2\text{DPB}$	370	515, 470–515 (sh)
$\text{Os}_2(\text{CH}_3)_2\text{DPB}$	367	442 (sh), 550 (sh)
$\text{Os}_2(p\text{-tolyl})_2\text{DPB}$	366	488, 530 (sh)
$\text{Os}_2(\text{C}_6\text{H}_3(\text{CF}_3)_2)_2\text{DPB}$	368	460–680 (sh)

solvents: CHCl_3 (7.26), $\text{C}_6\text{D}_5\text{H}$ (7.15), and $\text{C}_6\text{D}_6\text{CD}_2\text{H}$ (2.09). Variable-temperature experiments were calibrated by the frequency difference method with neat methanol under vacuum in a sealed NMR tube. UV-vis spectra were obtained with a Varian Cary 219 spectrophotometer or a Hewlett Packard 8450A diode array spectrometer. Mass spectra were obtained by the LSI ionization technique from the mass spectrometry facility of the University of California, San Francisco, for air-stable complexes.

Electrochemical experiments were performed in an inert atmosphere box using a Princeton Applied Research 175 wave generator and a 173 potentiostat/galvanostat. The working electrode (platinum disk, radius = 0.5 mm) was circumscribed by the platinum wire loop auxiliary electrode in a 2-mL compartment separated from the reference electrode by a luggin capillary. The pseudoreference electrode was a Ag wire and was referenced to ferrocene (FcP_2) at the end of the experiment. Because the data of reference potentials in THF were not available, potential conversions between reference and/or substrates were calculated approximately. It has been reported that $\text{FcP}_2^{+/0}$ is +0.31 V vs SCE in aprotic solvents, and SCE, in turn, is +0.24 V vs NHE in aqueous solutions.^{22,23} Thus, the relative conversion factor between the potential of $\text{FcP}_2^{+/0}$ and NHE was estimated as 0.55 V. Unless noted otherwise, all electrochemical experiments were carried out in THF with 0.2 M TBAPF₆ as the supporting electrolyte. The salt was recrystallized twice from ethanol, dried in a vacuum oven (10^{-2} Torr, 100 °C), and stored in the drybox. The metalloporphyrins were present in millimolar concentrations. Cyclic voltammograms were plotted in real time on an HPX-Y recorder. For the Hg-pool electrodes, electronic grade mercury was used. The Hg-pool electrodes were equipped with the mercury-pool working electrode, a platinum auxiliary electrode, and a pseudoreference electrode (Ag wire). Auxiliary and working electrodes were contacted with the reference electrode compartment by Luggin capillary. The working compartment of the electrochemical cell was closed with a rubber stopper, yielding about 10 mL of head space volume above the working solution. H_2 evolved from the electrocatalysis was kept in the head space of the cell until a sample was drawn by a Pressure-Lok gas syringe to be analyzed by GC. The solution was stirred with a magnetic stirrer during the electrocatalysis.

Detection of H_2 evolved via electrolyses was achieved utilizing an HP 5890 gas chromatograph with a thermal conductivity detector (TCD). A 12 ft stainless steel column packed with molecular sieves was activated with flowing Ar (30 mL/min, 250 °C, 24 h). For use, the column was held at 35–60 °C, the injection port at 40 °C, and the detector compartment at 50–60 °C. The carrier gas was high purity argon, flowing at a rate of 30 mL/min, and the retention times for H_2 and N_2 were 1 and 6 min, respectively. Reference samples of H_2 in N_2 were detected by GC quantitatively and showed approximate linearity with the concentration of H_2 over the range in which we were interested (from ca. 0.81% H_2/N_2 to ca. 1.61% H_2/N_2). Experimental samples (0.2 mL) were drawn into gas-tight syringes and injected into a GC.

Synthesis and Characterization of $\text{M}_2\text{R}_2\text{DPB}$ Complexes ($\text{M} = \text{Ru}$, Os ; $\text{R} = \text{CH}_3$, $p\text{-C}_6\text{H}_4\text{CH}_3$, $3,5\text{-(CF}_3)_2\text{C}_6\text{H}_3$) (see Tables IV and V for summaries of ^1H NMR and UV-vis data). (a) $[\text{Ru}_2^{\text{III/III}}\text{DPB}](\text{BF}_4)_2$ (1). The dimer dication was produced by using a procedure analogous to the literature procedure for $[\text{Ru}(\text{OEP})_2]^{2+}$.¹⁴ The Ru(II) dimer complex, Ru_2DPB (20 mg, 0.015 mmol), was dissolved in toluene (10

mL) in an inert atmosphere box under reduced lighting. An excess of AgBF_4 (7–10 mg, 1.2–1.7 times 2 equiv per dimer) was added to the dimer solution with stirring. Upon mixing the metalloporphyrin and the oxidant, a dark precipitate formed. After being stirred for 3 h, the mixture was filtered through a Celite pad. The Celite pad was carefully rinsed with toluene to remove excess AgBF_4 . CH_2Cl_2 was added to dissolve the dimer dication product and the Celite pad was washed thoroughly with CH_2Cl_2 until the filtrate became colorless. Gray Ag metal powder was left on the pad. This dimer dication was isolated from the CH_2Cl_2 solution by solvent evaporation. The spectral characteristics of this dimer dication, $[\text{Ru}_2\text{DPB}](\text{BF}_4)_2$, compared favorably with those of monomeric metalloporphyrin dimer analogs reported in the literature. $^1\text{H NMR}$ (CDCl_3 , ppm): H_{meso} 10.22 (s, 4H), 9.97 (s, 2H); $H_{\text{biphenylene}}$ 7.45 (d, 2H), 7.14 (2H), 6.76 (d, 2H); CH_2CH_3 4.85, 4.54, 4.20, 4.00 (m, 4H each); CH_3 3.90, 3.23 (s, 12H each), CH_2CH_3 1.48, 1.38 (t, 12H each). UV-vis (CH_2Cl_2 , λ_{max} (nm)): 350 (Soret), 380 (sh), 486 (sh), 518, 570 (sh), 636.

(b) $[\text{Os}_2^{\text{III}}(\text{DPB})](\text{BF}_4)_2$ (2). The dimer dication from the oxidation of Os_2DPB was produced by using the same method as the synthesis of $[\text{Ru}(\text{III})_2\text{DPB}](\text{BF}_4)_2$ described above. The $^1\text{H NMR}$ spectral characteristics of $[\text{Os}_2\text{DPB}](\text{BF}_4)_2$ were comparable to those of $[\text{Os}_2(\text{OEP})_2](\text{BF}_4)_2$ reported in the literature.¹⁴ $^1\text{H NMR}$ (CDCl_3 , ppm): H_{meso} 10.38 (s, 4H), 10.18 (s, 2H); $H_{\text{biphenylene}}$ 7.51 (d, 2H), 7.27 (t, 2H), 6.84 (d, 2H); CH_2CH_3 4.96, 4.65, 4.31, 4.15 (m, 4H each); CH_3 4.01, 3.32 (s, 12H each); CH_2CH_3 1.52, 1.44 (t, 12H each).

(c) $\text{Ru}_2(\text{CH}_3)_2\text{DPB}$ (3). In the drybox, the dimer dication, $[\text{Ru}_2\text{DPB}](\text{BF}_4)_2$, was suspended in Et_2O (10 mL) in a small round-bottom flask with a magnetic stir bar. Excess CH_3MgBr in Et_2O (more than 2 equiv per $[\text{Ru}_2\text{DPB}](\text{BF}_4)_2$) was added dropwise with stirring. Upon addition of the Grignard reagent, a soluble red product formed and thus the solution became red immediately. After being stirred for 1 h, the soluble part was separated and the solid which did not react with CH_3MgBr was treated with the Grignard reagent again in Et_2O . The red solution from the second treatment was combined with the first one and the solvent was removed by vacuum. The product was flash chromatographed on a silica column (1 × 15 cm, hexanes:benzene = 2:1) to yield purified $\text{Ru}_2(\text{CH}_3)_2\text{DPB}$ (15 mg from 19 mg of Ru_2DPB , 77%).

(d) $\text{Ru}_2(p\text{-C}_6\text{H}_4\text{CH}_3)_2\text{DPB}$ (4). The $\text{Ru}_2(p\text{-tolyl})_2\text{DPB}$ complex was synthesized from the dimer dication, $[\text{Ru}_2\text{DPB}](\text{BF}_4)_2$, by the experimental procedure described above. $p\text{-CH}_3\text{C}_6\text{H}_4\text{MgBr}$ (0.1 M in Et_2O) was used as the Grignard reagent to treat the dimer dication. This compound was also purified by flash column chromatography (SiO_2 , 1 × 12 cm, hexanes:benzene = 1.5:1) in the drybox. This compound was found to be air-stable in a benzene solution for days. LSIMS: $m/e = 1486$, cluster, M^+ .

(e) $\text{Ru}_2(3,5\text{-}(\text{CF}_3)_2\text{C}_6\text{H}_3)_2\text{DPB}$ (5). The Grignard reagent used here was made following a procedure described in the literature.³⁴ In the drybox, Mg (24 mg, 1 mmol, granular, 20 mesh) was placed in Et_2O (5 mL) in a scintillation vial. $3,5\text{-}(\text{CH}_3)_2\text{C}_6\text{H}_3\text{Br}$ (0.15 mL) was dissolved in Et_2O (3 mL) in another vial. This aryl bromide solution was slowly added to the ethereal Mg suspension with stirring. The reaction was initiated with heat and the solution first became yellow and then brown. The solution was stirred for several hours, after which no Mg metal was left. This $3,5\text{-}(\text{CH}_3)_2\text{C}_6\text{H}_3\text{MgBr}/\text{Et}_2\text{O}$ solution was used for the next reaction without further purification or quantification.

The $\text{Ru}_2(3,5\text{-}(\text{CF}_3)_2\text{C}_6\text{H}_3)_2\text{DPB}$ complex was synthesized from the dimer dication and the corresponding Grignard reagent prepared above. The product was purified by flash column chromatography (SiO_2 , 1 × 14 cm, hexanes:benzene = 2:1) in the drybox (6.3 mg from 8 mg of Ru_2DPB , 59%). This compound was air-stable in benzene solution for days. LSIMS: $m/e = 1729$, cluster, M^+ .

(f) $\text{Os}_2(\text{CH}_3)_2\text{DPB}$ (6). $\text{Os}_2(\text{R})_2\text{DPB}$ complexes were synthesized by using the same procedures used for $\text{Ru}_2(\text{R})_2\text{DPB}$ complexes. The dimer dication, $[\text{Os}_2\text{DPB}](\text{BF}_4)_2$ (10 mg, 0.006 mmol), was suspended in Et_2O (10 mL) and excess CH_3MgBr in Et_2O was added dropwise with stirring. Upon addition of the Grignard reagent, the reaction mixture turned red brown. After being stirred for 30 min, the soluble part was separated

and the solid which had not reacted with the Grignard reagent was treated with CH_3MgBr in Et_2O again. This second solution was combined with the first one and the solvent was removed by vacuum. The product was flash chromatographed (SiO_2 , 1 × 15 cm, hexanes:benzene = 2.5:1) and the leading red brown band was collected and dried under vacuum (14 mg from 10 mg of $[\text{Os}_2\text{DPB}](\text{BF}_4)_2$, 76%).

(g) $\text{Os}_2(p\text{-C}_6\text{H}_4\text{CH}_3)_2\text{DPB}$ (7). The $\text{Os}_2(p\text{-CH}_3\text{C}_6\text{H}_4)_2\text{DPB}$ complex was synthesized from the dimer dication, $[\text{Os}_2\text{DPB}](\text{BF}_4)_2$, by the experimental procedure described above. An excess of $p\text{-CH}_3\text{C}_6\text{H}_4\text{MgBr}$ in Et_2O was treated with the dimer dication. The product was purified by flash column chromatography (SiO_2 , 1 × 15 cm, hexanes:benzene = 2:1) in the drybox.

(h) $\text{Os}_2(3,5\text{-}(\text{CF}_3)_2\text{C}_6\text{H}_3)_2\text{DPB}$ (8). The $\text{Os}_2(3,5\text{-}(\text{CF}_3)_2\text{C}_6\text{H}_3)_2\text{DPB}$ complex was synthesized from the dimer dication and the Grignard reagent, $3,5\text{-}(\text{CF}_3)_2\text{C}_6\text{H}_3\text{MgBr}$, in Et_2O prepared as described above. The product was purified by flash column chromatography (SiO_2 , 1 × 15 cm, hexanes:benzene = 2:1) in the drybox (8.5 mg from 13.7 mg of Os_2DPB , 48%).

(i) $\text{Os}^{\text{IV}}_2(\text{O})(p\text{-C}_6\text{H}_4\text{CH}_3)_2\text{DPB}$ (9) (μ -oxo-bis(p -tolyl)diosmium diporphyrinatobiphenylene). When an $\text{Os}^{\text{III}}_2(p\text{-CH}_3\text{C}_6\text{H}_4)_2\text{DPB}$ solution in benzene was exposed to air, the solution color changed from red brown to dark green. After being stirred overnight in air, the solution was evaporated and dried under vacuum. $^1\text{H NMR}$ (C_6D_6 , ppm): H_{meso} 9.34 (s, 2H), 9.13 (s, 4H); $H_{\text{biphenylene}}$ 7.02 (d, 2H), 6.95 (d, 2H), 6.80 (t, 2H); CH_2CH_3 4.24, 3.84 (m, 8H each); CH_3 3.38, 3.24 (s, 12H each); CH_2CH_3 1.83, 1.61 (t, 12H each, 7.5 Hz); p -tolyl H_m 3.93 (d, 4H, 8 Hz), p - CH_3 0.17 (s, 6H), H_o -0.40 (d, 4H, 8 Hz). UV-vis (toluene, λ_{max} (nm)): 374 (Soret), 510 (sh). LSIMS: $m/e = 1680$, cluster, M^+ ; 1589, cluster, $\text{M}^+ - \text{C}_6\text{H}_4\text{CH}_3$.

(j) $\text{Os}^{\text{IV}}_2(\text{O})(3,5\text{-}(\text{CF}_3)_2\text{C}_6\text{H}_3)_2\text{DPB}$ (10) (μ -oxo-bis(3,5-bis(trifluoromethyl)phenyl)diosmium diporphyrinatobiphenylene). When an $\text{Os}^{\text{III}}_2(3,5\text{-}(\text{CF}_3)_2\text{C}_6\text{H}_3)_2\text{DPB}$ solution in benzene was exposed to air, the solution color changed from brown to dark green. After being stirred overnight in air, the solution was evaporated and dried under vacuum. $^1\text{H NMR}$ (C_6D_6 , ppm): H_{meso} 9.52 (s, 2H), 9.10 (s, 4H); $H_{\text{biphenylene}}$ 7.24 (d, 2H), 7.03 (d, 2H), 6.87 (t, 2H); CH_2CH_3 4.29, 4.05, 3.84, 3.71 (m, 4H each); CH_3 3.28, 3.25 (s, 12H each); CH_2CH_3 1.83, 1.49 (t, 12H each, 7.6 Hz); $\text{C}_6\text{H}_3(\text{CF}_3)_2$ H_p 4.95 (s, 2H), H_o -0.26 (s, 4H). UV-vis (toluene, λ_{max} (nm)): 374 (Soret), 490 (sh). LSIMS: $m/e = 1924$, cluster, M^+ ; 1304, cluster, $\text{M}^+ - 2\text{C}_6\text{H}_3(\text{CF}_3)_2$.

$[\text{M}_2\text{R}_2\text{DPB}]^{2-}$. All the dianions of $\text{M}_2\text{R}_2\text{DPB}$ ($\text{M} = \text{Ru}, \text{Os}$; $\text{R} = \text{CH}_3$, $3,5\text{-}(\text{CF}_3)_2\text{C}_6\text{H}_3$) were prepared by quantitative titration of the neutral $\text{M}_2\text{R}_2\text{DPB}$ species with 2 equiv of $\text{K}^+\text{C}_{10}\text{H}_8^-$. The end point of each titration was detected with the distinctive color change of the solution from brown-red to green-brown. As discussed above, another diamagnetic reduced species which displays a slightly different but complete set of proton resonances was sometimes detected.

(k) $[\text{Ru}_2(\text{CH}_3)_2\text{DPB}]^{2-}$ (11) $^1\text{H NMR}$ ($\text{THF-}d_8$, ppm): H_{meso} and $H_{\text{biphenylene}}$ 7.65–6.71; CH_2CH_3 3.20, 3.07 (m, 16H total); CH_3 2.86, 2.66 (s, 12H each); CH_2CH_3 1.43, 1.37 (t, 12H each); $\text{Ru}-\text{CH}_3$ -9.25 (s, 6H).

(l) $[\text{Os}_2(\text{CH}_3)_2\text{DPB}]^{2-}$ $^1\text{H NMR}$ ($\text{THF-}d_8$, ppm): $H_{\text{biphenylene}}$ 7.25–6.90; H_{meso} 6.51 (s, 4H), 6.31 (s, 2H); CH_3 3.01, 2.99 (s, 12H each); CH_2CH_3 3.4–3.1 (m, 16H total); CH_2CH_3 1.34, 1.32 (t, 12H each); $\text{Os}-\text{CH}_3$ -12.48 (s, 6H).

(m) $[\text{Ru}_2(\text{C}_6\text{H}_3(\text{CF}_3)_2)_2\text{DPB}]^{2-}$ (13) $^1\text{H NMR}$ ($\text{THF-}d_8$, ppm): H_{meso} 8.28 (s, 2H), 7.97 (s, 4H); $H_{\text{biphenylene}}$ 7.14 (d, 2H), 6.95 (t, 2H), 6.89 (d, 2H); CH_2CH_3 3.27 (q, 16H total); CH_3 3.01, 2.73 (s, 12H each); CH_2CH_3 1.41 (t, 24H total); H_p 5.13 (s, 2H); H_o 2.10 (s, 4H).

(n) $[\text{Os}_2(\text{C}_6\text{H}_3(\text{CF}_3)_2)_2\text{DPB}]^{2-}$ (14) $^1\text{H NMR}$ ($\text{THF-}d_8$, ppm): H_{meso} and $H_{\text{biphenylene}}$ 7.39–6.52; CH_2CH_3 3.3–3.2 (m, 16H total); CH_3 3.10–2.85 (s, 12H each); CH_2CH_3 and H_o 1.4–1.2; H_p 5.5 (s, 2H). These proton resonances in 14 were sometimes too obscure to be assigned for certain.

Acknowledgment. We thank the National Science Foundation (CHE9123187) for financial support and L.L. Chng for repeating some experiments. Measurement of mass spectra by the Mass Spectrometry Facility, University of California, San Francisco, supported by the NIH Division of Research Resources (Grant No. RR01614) is acknowledged. Y.H.'s portion of this work is dedicated to her parents (Prof. Y.G. Ha and K.S. Lee) on the occasion of her father's 60th birthday.

(34) Pavia, D. L.; Lampman, G. M.; Kriz, G. S., Jr. *Introduction to Organic Laboratory Techniques*; W. B. Saunders: Philadelphia, 1976; p 219.

(35) From Table of Weak Acid Dissociation Constants in: Poiss, L. W. *Quantitative Analysis*; Harper & Row: New York, 1987.